

1-1-1994

Spectral signature of quantum spin diffusion in dimensions $d = 1, 2, \text{ and } 3$

Markus Böhm

Hajo Leschke

Martin Henneke

V. S. Viswanath

University of Rhode Island

Joachim Stolze

University of Rhode Island

See next page for additional authors

Follow this and additional works at: https://digitalcommons.uri.edu/phys_facpubs

Citation/Publisher Attribution

Markus Böhm, Hajo Leschke, Martin Henneke, V.S. Viswanath, Joachim Stolze and Gerhard Müller.
Spectral signature of quantum spin diffusion in dimensions $d=1,2,3$. Phys. Rev. B **49** (1994), 417-421.
Available at: <http://journals.aps.org/prb/abstract/10.1103/PhysRevB.49.417>

This Article is brought to you by the University of Rhode Island. It has been accepted for inclusion in Physics Faculty Publications by an authorized administrator of DigitalCommons@URI. For more information, please contact digitalcommons-group@uri.edu. For permission to reuse copyrighted content, contact the author directly.

Spectral signature of quantum spin diffusion in dimensions $d = 1, 2,$ and 3

Publisher Statement

Copyright 1994 The American Physical Society.

Authors

Markus Böhm, Hajo Leschke, Martin Henneke, V. S. Viswanath, Joachim Stolze, and Gerhard Müller

Terms of Use

All rights reserved under copyright.

Spectral signature of quantum spin diffusion in dimensions $d = 1, 2,$ and 3

Markus Böhm and Hajo Leschke

Institut für Theoretische Physik, Universität Erlangen-Nürnberg, D-91058 Erlangen, Germany

Martin Henneke

Physikalisch-Technische Bundesanstalt, Abt. 8.1, D-38116 Braunschweig, Germany

V. S. Viswanath, Joachim Stolze,* and Gerhard Müller

Department of Physics, University of Rhode Island, Kingston, Rhode Island 02881-0817

(Received 23 July 1993)

The spectral densities of dynamical spin autocorrelation functions at infinite temperature are studied for the $S = \frac{1}{2} XXZ$ model (with exchange couplings $J_x = J_y \equiv J, J_z$) on the linear chain, the square lattice, and the simple cubic lattice. The low-frequency behavior of a given spectral density is inferred from certain characteristic properties of its continued-fraction coefficients as determined from computed frequency moments. The analysis yields estimates for the J_z/J dependence of the infrared-singularity exponent. In the $d = 1$ case, the exponent for spin fluctuations perpendicular to the $O(2)$ symmetry axis responds sensitively as the anisotropy parameter sweeps across the $O(3)$ symmetry point $J_z/J = 1$, while the exponent for the parallel fluctuations shows little variation. In the cases $d = 2$ and $d = 3$ the same observations are made for autocorrelation functions of aggregate spins in chains and lattice planes, respectively.

I. INTRODUCTION

The phenomenological concept of diffusion of a conserved magnetization component was introduced more than four decades ago.¹ It has been very useful for the interpretation of experiments that probe the transport of spin fluctuations at high temperature. However, a genuinely microscopic theory of spin diffusion has remained a challenge for theorists to this day. For classical spin models, the most detailed results on spin diffusion are being produced by simulation studies. But in spite of considerable computational investments, no consensus has emerged yet, for example, on the exact nature of the long-time behavior of spin autocorrelation functions at infinite temperature for the Heisenberg model.^{2,3} In quantum spin systems, the characteristic signatures of spin diffusion have for the most part eluded detection beyond ambiguity until recently, when new techniques for the analysis of frequency moments^{4,5} or the corresponding continued-fraction coefficients^{6,7} were introduced.

Here we study $T = \infty$ autocorrelation functions of spin operators for the $S = \frac{1}{2} XXZ$ model

$$H_{XXZ} = - \sum_{\langle i,j \rangle} \{J(S_i^x S_j^x + S_i^y S_j^y) + J_z S_i^z S_j^z\}, \quad (1)$$

with nearest-neighbor coupling on a linear chain ($d = 1$), a square lattice ($d = 2$), or a simple cubic lattice ($d = 3$). The z component S_T^z of the total spin is conserved for arbitrary values of J_z/J , but S_T^z only for the isotropic case $J_z/J = 1$ (Heisenberg model). The variation of the continuous parameter J_z/J switches one conservation law on and off at the symmetry point while the other one stays

on all the way. Diffusive behavior of a given spin component, for which the conservation law is a prerequisite, manifests itself as a characteristic long-time tail, $\propto t^{-d/2}$, in the local spin autocorrelation function. This corresponds to a characteristic infrared (i.e., low-frequency) singularity in the spectral density.

The continued-fraction analysis of spectral densities as previously developed and used in the context of the recursion method^{8,9} offers some very sensitive instruments for the determination of precisely that infrared singularity.

II. METHOD

We consider a normalized spin autocorrelation function at $T = \infty$ for a site on an infinite lattice,

$$C^{\mu\mu}(t) = \frac{\langle S_0^\mu(t) S_0^\mu \rangle}{\langle S_0^\mu S_0^\mu \rangle}, \quad \mu = x, z, \quad (2)$$

and the corresponding spectral density

$$\Phi^{\mu\mu}(\omega) = \int_{-\infty}^{\infty} dt e^{i\omega t} C^{\mu\mu}(t). \quad (3)$$

The correlation function can be expanded into a power series of the form

$$C^{\mu\mu}(t) = \sum_{k=0}^{\infty} \frac{(-1)^k}{(2k)!} M_{2k}^{\mu\mu} t^{2k}, \quad (4)$$

where the expansion coefficients are the frequency moments of the spectral density,

$$M_{2k}^{\mu\mu} = \int_{-\infty}^{\infty} \frac{d\omega}{2\pi} \omega^{2k} \Phi^{\mu\mu}(\omega), \quad (5)$$

and can be expressed as expectation values of iterated commutators involving the Hamiltonian H_{XXZ} and the spin operator S_0^μ . The evaluation of the moments is straightforward in principle but exceedingly tedious in practice — an ideal task for computers.^{4,5,10–13}

The short-time expansion (4) is obviously not suited to study a long-time phenomenon such as diffusion. However, the information contained in the first K frequency moments (5) may be put to work by converting them into the first K continued-fraction coefficients $\Delta_k^{\mu\mu}$ of the relaxation function¹⁴

$$c^{\mu\mu}(z) = \int_0^\infty dt e^{-zt} C^{\mu\mu}(t) = \frac{1}{z + \frac{\Delta_1^{\mu\mu}}{z + \frac{\Delta_2^{\mu\mu}}{z + \dots}}} . \quad (6)$$

In a typical application, the sequence of continued-fraction coefficients $\Delta_k^{\mu\mu}$ displays patterns which reflect characteristic properties of the spectral density (3). One of these recognizable patterns is directly related to the exponent of the infrared singularity in $\Phi^{\mu\mu}(\omega)$, as we shall see.

An important characteristic of a sequence of continued-fraction coefficients is its growth rate. It is defined as the power of k with which a given Δ_k sequence grows on average (asymptotically):

$$\Delta_k^{\mu\mu} \propto k^\lambda. \quad (7)$$

The growth rate determines the decay law of the spectral density (3) at high frequencies:^{15,16}

$$\Phi^{\mu\mu}(\omega) \propto e^{-|\omega|^{2/\lambda}}. \quad (8)$$

The available data for the XXZ model exhibit growth rates in the range $1 \lesssim \lambda \lesssim 2$.

Our method of estimating the infrared-singularity exponent in $\Phi^{\mu\mu}(\omega)$ proceeds as follows: We choose a model spectral density with (i) a variable overall frequency scale unit ω_0 , (ii) a power-law infrared singularity with variable exponent α , and (iii) a high-frequency decay law of the type (8) with variable growth rate λ . The simplest function which meets these requirements and has the correct normalization reads

$$\Phi(\omega) = \frac{2\pi}{\lambda\omega_0\Gamma[\frac{\lambda}{2}(1+\alpha)]} \left| \frac{\omega}{\omega_0} \right|^\alpha \exp\left(-\left| \frac{\omega}{\omega_0} \right|^{2/\lambda}\right). \quad (9)$$

The frequency moments of this spectral density are

$$M_{2k} = \omega_0^{2k} \frac{\Gamma[\frac{\lambda}{2}(1+\alpha+2k)]}{\Gamma[\frac{\lambda}{2}(1+\alpha)]}. \quad (10)$$

Closed-form expressions for the corresponding continued-fraction coefficients are only known for the special case $\lambda = 1$:

$$\Delta_{2k-1} = \frac{1}{2}\omega_0^2(2k-1+\alpha), \quad \Delta_{2k} = \frac{1}{2}\omega_0^2(2k). \quad (11)$$

Here the singularity exponent α can be determined from the vertical displacement of the Δ_{2k-1} from the line Δ_{2k} . For $\lambda \neq 1$, a singularity of growing strength in (9) still causes an alternating pattern of growing amplitude in Δ_k , but the relation between exponent and displacement is more complicated. Looking at our data for the XXZ model, we observe that the characteristic alternating pattern is most conspicuously present in the $\Delta_k^{\mu\mu}$ sequences precisely in those cases where a diffusive infrared singularity is expected to dominate the low-frequency behavior of $\Phi^{\mu\mu}(\omega)$.

The known coefficients Δ_k^{xx} of $\Phi^{xx}(\omega)$ for $J_z/J = 1$ and $J_z/J = 0.3$ are displayed vs k in the main plot of Fig. 1 (circles connected by solid lines). Note the different growth rates and degrees of alternation. In order to estimate the exponent value $\alpha_{\mu\mu}$ that gives rise to the observed amount of alternation in the data sequence $\Delta_1^{\mu\mu}, \dots, \Delta_K^{\mu\mu}$, we determine a matching model sequence $\Delta_1, \dots, \Delta_K$ obtained from (10) by numerically minimizing the mean-square deviation

$$\sum_{k=k_{\min}}^K (\Delta_k^{\mu\mu} - \Delta_k)^2 \quad (12)$$

with respect to the undetermined parameters λ , α , and ω_0 . The lower cutoff k_{\min} was found to be necessary because the first few continued-fraction coefficients tend to deviate significantly from the asymptotic behavior described by the model coefficients Δ_k . We have set $k_{\min} = 3$ for all sequences analyzed here. Two optimized model Δ_k sequences are displayed as dashed lines in Fig. 1 along with the data sets to which they have been fitted.

We know the exact moments $M_{2k}^{\mu\mu}$ up to $K = 14, 7, 6$ in $d = 1, 2, 3$ space dimensions, respectively.¹⁷ The growth

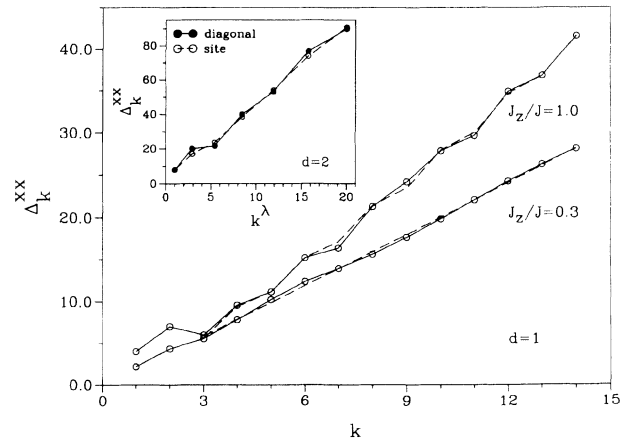


FIG. 1. Continued-fraction coefficients $\Delta_1^{xx}, \dots, \Delta_{14}^{xx}$ (circles connected by solid lines) of the xx site-spin autocorrelation function at $T = \infty$ for two cases of the XXZ chain. The sequences for $J_z/J = 0.3$ and 1.0 have growth rates $\lambda = 1.03$ and $\lambda = 1.18$, respectively. The model Δ_k sequences which provide the best fit as described in the text are shown as dashed lines. The inset shows the Δ_k^{xx} plotted vs k^λ for the site spin (open circles) and the (diagonal) chain spin (solid circles) of the $S = \frac{1}{2}$ XXZ model at $T = \infty$ on the square lattice. Here $\lambda = 1.54$ is the growth rate of the site-spin data.

rates λ range between 1.0 and 1.3 for $d = 1$ and up to 2.0 for $d = 2$ and 3.¹⁸

Before the presentation of our results, let us briefly review the predictions of diffusion phenomenology. The Green function of the d -dimensional diffusion equation (with Dirichlet boundary conditions at infinity) is given by

$$G(\mathbf{r}, t) = \frac{e^{-r^2/4Dt}}{(4\pi Dt)^{d/2}}, \quad (13)$$

where D is the diffusion constant. This function describes the density of a diffusing (globally conserved) quantity initially concentrated in a point at the origin. The density autocorrelation function of that quantity exhibits the characteristic diffusive long-time tail: $G(\mathbf{0}, t) \propto t^{-d/2}$. Integration of the d -dimensional Green function over one spatial coordinate yields the $(d-1)$ -dimensional Green function. Physically, this describes the diffusive spreading of a linelike distribution. A planelike initial distribution is obtained by integrating over two dimensions. The spectral density of $G(\mathbf{0}, t)$ has infrared singularities of the form $\sim |\omega|^{-1/2}$, $\sim \ln|\omega|$, and $\sim |\omega|^{1/2}$ in $d = 1, 2, 3$, respectively. Our method of analysis is sensitive mainly to the strongest of these three singularities, $\sim |\omega|^{-1/2}$. That singularity is expected for site-spin autocorrelation functions in $d = 1$ as well as for autocorrelation functions of chainlike and lattice-plane spin aggregates in $d = 2$ and 3, respectively.

In more general terms, the idea behind our method of analysis may be stated as follows: Associated with any d -dimensional diffusion process on a d -dimensional lattice is a one-dimensional diffusion process on the same lattice, described in terms of aggregate dynamical variables. Therefore, the alternating pattern in the $\Delta_k^{\mu\mu}$ data, which is a direct and sensitive indicator of one-dimensional diffusion processes, is at the same time an indirect but equally sensitive indicator of d -dimensional diffusion processes for $d > 1$.

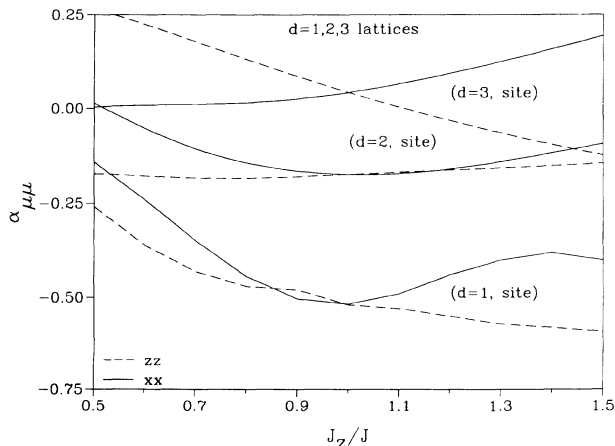


FIG. 2. J_z/J dependence of the infrared exponents α_{xx} (solid lines) and α_{zz} (dashed lines) for the site-spin spectral densities at $T = \infty$ of the $S = \frac{1}{2}$ XXZ model in lattice dimensions $d = 1, 2, 3$.

III. RESULTS

The J_z/J dependence of the infrared exponents α_{xx} and α_{zz} for the autocorrelation functions of a site spin on a lattice of dimension $d = 1, 2, 3$ is displayed in Fig. 2. We see at one glance that our indicator detects fairly reliably where site-spin autocorrelation functions describe one-dimensional diffusion, namely, for the $d = 1$ lattice only. The exponent α_{xx} varies strongly with J_z/J as expected and assumes a minimum value at the symmetry point $J_z/J = 1$, consistent with $d = 1$ spin diffusion. The exponent α_{zz} , by contrast, stays near that value over the entire anisotropy range shown, thus reflecting sustained diffusive behavior.^{19,20} The broad nature of the minimum in α_{xx} is attributable to the fact that the true long-time behavior is only nebulously encoded in the first few continued-fraction coefficients.

The data for the site-spin exponents α_{xx} and α_{zz} in lattice dimensions $d = 2, 3$ lie significantly above the $d = 1$ data. In $d = 2$, site-spin diffusion is characterized by a logarithmic divergence in the spectral density. That weak divergence causes a shallow minimum in α_{xx} at $J_z/J = 1$ and a sustained negative α_{zz} of much smaller magnitude than in $d = 1$. The characteristic $\sim |\omega|^{1/2}$ cusp singularity of $d = 3$ site-spin diffusion is unlikely to be detectable by our analysis because of terms in the spectral density that are regular at $\omega = 0$. Our data for α_{xx} and α_{zz} , which are non-negative except near the margins, indeed do not bear any signature of the diffusive cusp singularity.

The exponents α_{xx} and α_{zz} for the $d = 1$ case were previously analyzed by a somewhat different method,⁷ which does not take fully into account the deviations of the growth rate from unity. That gave rise to significant systematic errors in the resulting exponent values. They have been much reduced in the results of the present method.

Figures 3 and 4 summarize our numerical evidence for

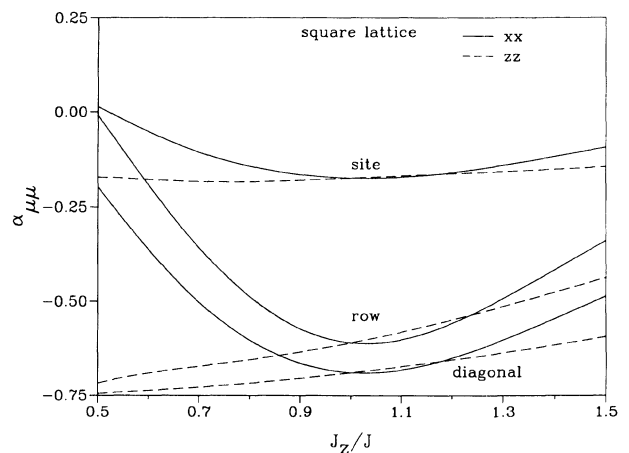


FIG. 3. J_z/J dependence of the infrared exponents α_{xx} (solid lines) and α_{zz} (dashed lines) for three types of spectral densities at $T = \infty$ of the $S = \frac{1}{2}$ XXZ model on the square lattice: site spin, chain spins in (1 0) direction (row), and (1 1) direction (diagonal).

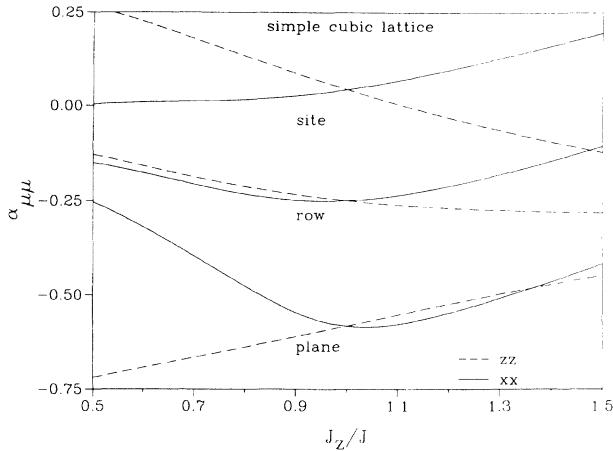


FIG. 4. J_z/J dependence of the infrared exponents α_{xx} (solid lines) and α_{zz} (dashed lines) for three types of spectral densities at $T = \infty$ of the $S = \frac{1}{2}$ XXZ model on the simple cubic lattice: site spin, chain spin in $(1\ 0\ 0)$ direction (row), and $(1\ 0\ 0)$ plane spin.

quantum spin diffusion in lattice dimensions $d = 2, 3$. Consider first the square lattice (Fig. 3). The two uppermost curves, which we have already discussed in the context of Fig. 2, reflect the weak logarithmic divergence in $\Phi^{\mu\mu}(\omega)$ associated with the *two-dimensional* site-spin diffusion. The two pairs of curves underneath bear the signature of the much stronger $\omega^{-1/2}$ divergence in $\Phi^{\mu\mu}(\omega)$ associated with the *one-dimensional* diffusion of chainlike spin aggregates consisting of entire rows or diagonals of spins on the lattice. The exponent α_{xx} now has a much deeper minimum at $J_z/J = 1$, and α_{zz} stays strongly negative over the entire parameter range.

The difference between the results for the two types of chain spins in Fig. 3 is attributable to the fact that the $\Delta_k^{\mu\mu}$ used in our analysis to gain information on the isotropic long-time dynamics are strongly influenced by the anisotropic short-time dynamics. The deviations between the two sets of curves are non-negligible but sufficiently small to make our approach meaningful.

The different strengths of infrared divergence in the site-spin and chain-spin spectral densities at $J_z/J = 1$ are already detectable in the corresponding continued-fraction coefficients Δ_k^{xx} as displayed in the inset to Fig. 1 by their different amplitudes of even-odd alternation.

On the simple cubic lattice (Fig. 4), we investigate one-, two-, and three-dimensional diffusion processes. The two curves at the top represent the infrared exponents for the site-spin spectral densities, which are, as already stated in the context of Fig. 2, largely insensitive to the $\sim \omega^{1/2}$ cusp singularity associated with *three-dimensional* spin diffusion. The two curves in the middle of Fig. 4 resemble those at the top of Fig. 3 insofar as both sets reflect the weak divergence of *two-dimensional* spin diffusion, chain-spin diffusion on the cubic lattice and site-spin diffusion on the square lattice, respectively. Likewise, the two curves at the bottom of Fig. 4, which describe the infrared exponents of lattice-plane spin spectral densities for the $d = 3$ lattice, exhibit the same characteristic signature of *one-dimensional* spin diffusion as did the exponents of chain-spin spectral densities for the $d = 2$ lattice (Fig. 3) and the site-spin spectral densities for the $d = 1$ lattice (Fig. 2).

In conclusion, our method of analysis makes it possible to identify quantum spin diffusion processes in lattice dimensions $d = 1, 2, 3$ and to discriminate between diffusion processes of different dimensionality on a given ($d \geq 2$) lattice.

ACKNOWLEDGMENTS

The work done at URI was supported by the U.S. National Science Foundation, Grants Nos. DMR-90-07540 and DMR-93-12252. Computations were carried out on supercomputers at the National Center for Supercomputing Applications, University of Illinois at Urbana-Champaign. J.S. gratefully acknowledges support by the Max Kade Foundation. M.B. wishes to thank the Studienstiftung des deutschen Volkes for support.

* On leave from Institut für Physik, Universität Dortmund, D-44221 Dortmund, Germany.

¹ N. Bloembergen, *Physica* **15**, 386 (1949).

² G. Müller, *Phys. Rev. Lett.* **60**, 2785 (1988); **63**, 813 (1989); R.W. Gerling and D.P. Landau, *ibid.* **63**, 812 (1989); *Phys. Rev. B* **42**, 8214 (1990); O.F. de Alcantara Bonfim and G. Reiter, *Phys. Rev. Lett.* **69**, 367 (1992); **70**, 249 (1993); M. Böhm, R.W. Gerling, and H. Leschke, *ibid.* **70**, 248 (1993).

³ N. Srivastava, V.S. Viswanath, J.-M. Liu, and G. Müller, *J. Appl. Phys.* (to be published).

⁴ M. Böhm and H. Leschke, *J. Phys. A* **25**, 1043 (1992).

⁵ M. Böhm and H. Leschke, *Physica A* **199**, 116 (1993).

⁶ J. Stolze, V.S. Viswanath, and G. Müller, *Z. Phys. B* **89**, 45 (1992).

⁷ M. Böhm, V.S. Viswanath, J. Stolze, and G. Müller (unpublished).

⁸ V.S. Viswanath and G. Müller (unpublished).

⁹ V.S. Viswanath and G. Müller, *J. Appl. Phys.* **67**, 5486

(1990); **70**, 6178 (1991).

¹⁰ T. Morita, *J. Math. Phys.* **12**, 2062 (1971).

¹¹ J.M.R. Roldan, B.M. McCoy, and J.H.H. Perk, *Physica A* **136**, 255 (1986).

¹² U. Brandt and J. Stolze, *Z. Phys. B* **64**, 327 (1986).

¹³ J. Stolze and U. Brandt, *Z. Phys. B* **77**, 111 (1989).

¹⁴ A simple and numerically stable algorithm was presented in Refs. 7 and 8.

¹⁵ A. Magnus, in *The Recursion Method and its Applications*, edited by D.G. Pettifor and D.L. Weaire (Springer-Verlag, New York, 1985), p. 22.

¹⁶ D.S. Lubinsky, *Acta Appl. Math.* **10**, 237 (1987).

¹⁷ Some of the frequency moments on which our analysis is based can be found in the literature, specifically in Refs. 4 and 7 for $d = 1$, in Ref. 13 for $d = 2$, and in Ref. 10 for $d = 3$. The additional moments determined for this study are available from the authors.

¹⁸ Growth rates $\lambda \geq 2$ are known to cause some mathematical problems: The continued fraction (6) no longer

converges and the spectral density (3) can no longer be uniquely reconstructed from its (infinitely many) moments or continued-fraction coefficients. However, these problems do not jeopardize the exponent analysis of the present study.

¹⁹ For the $d = 1$ model the analysis of the exponent α_{zz} becomes inapplicable in the parameter range $0 \leq J_z/J \lesssim 0.6$ because of a crossover in growth rate which is related to the free-fermion nature of that system at $J_z/J = 0$ (see

Ref. 7 for further details on that aspect).

²⁰ A similar J_z/J dependence of the infrared exponents has been obtained for the $d = 1$ XXZ models with $S = 1$ and $S = \infty$ (classical spins), however with considerably stronger deviations from the expected dominant patterns in both the $\Delta_k^{\mu\mu}$ sequences and the $\alpha_{\mu\mu}$. For these two systems we know $K = 9$ and $K = 8$ exact moments, respectively (see Ref. 5).